Corneal Complications in Streptozocin-Induced Type I Diabetic Rats

Jia Yin, Jenny Huang, Cynthia Chen, Nan Gao, Feng Wang, and Fu-Shin X. Yu

Purpose. This study seeks to characterize corneal functions and complications in a streptozocin (STZ)-induced rat model of type I diabetes mellitus (DM) and to understand the pathogenesis of diabetic keratopathy.

Methods. DM was induced via STZ injection in Sprague-Dawley rats. Body weight, length, and corneal size were measured and compared with the age-matched normal controls. Corneal morphology and histology were evaluated with slit lamp, digital confocal microscopy and hematoxylin and eosin staining. Tear secretion was measured with cotton threads, and corneal sensitivity was determined with an esthesiometer. Protein expression and distribution were assessed with Western blotting and immunohistochemistry. Wound healing was determined using an in vivo corneal epithelial debridement model.

Results. Compared with the normal control rats, STZ rats had reduced body weight, and body length, but minimally affected corneal size. No significant changes in ocular surface regularity, corneal thickness, and morphology were noted in diabetic corneas. STZ rats showed stronger Rose Bengal staining, decreased tear secretion, slightly attenuated sensitivity, less innervation, delayed epithelial wound healing, and impaired epidermal growth factor receptor signaling in their corneas. While the expression of adherens junction protein β-catenin, and tight junction proteins occludin and ZO-1 was unchanged, the formation of these junctions after wound closure was delayed.

Conclusions. Pathogenesis of diabetic keratopathy involves multiple tissues and/or cell types and several events including reduced tear secretion, impaired innervation, weakened cell junction, and altered wound responses. These insights may prove useful for the clinical translation of evolving strategies for the management and treatment of diabetic corneal complications. (*Invest Ophthalmol Vis Sci.* 2011;52:6589–6596) DOI:10.1167/iovs.11-7709

With rapid increases in the prevalence of diabetes mellitus (DM) worldwide, ocular complications have become a leading cause of blindness.[1] In addition to the abnormalities of the retina (retinopathy) and the lens (cataract), various types of corneal disorders, collectively termed diabetic keratopathy (DK), are also relatively common in persons with DM.[2,3] Reduced tear production,[4–6] decreased corneal sensitivity and innervation,[6–9] changes in endothelial morphology and function,[10] alterations of corneal epithelial basement membrane,[11] and increased corneal thickness[12–14] have been documented in diabetic patients. Streptozocin (STZ)-induced diabetes has long been used as an animal model for type I DM study. Systematical characterization of the health status of the ocular surface and the functions of the cornea in this model has been incomplete.

In addition to the aforementioned complications, delayed corneal epithelial wound healing is also common in diabetic corneas and may compromise patient's vision. Particularly for diabetic retinopathy patients undergoing vitrectomy, the removal of corneal epithelium during the procedure results in a considerable delay in re-epithelialization.[2,3,15,16] Delayed epithelial healing predisposes patients to sight-threatening complications, such as stromal opacification, surface irregularity, and microbial keratitis. DK and delayed wound healing may also cause persistent epithelial defects and recurrent erosion, two painful and hard to treat conditions.[3] Therefore delineating the underlying mechanisms of delayed healing is of great importance in maintaining corneal integrity in diabetic patients.

Alterations in the epithelial basement membrane,[17,18] lack of sufficient tear secretion,[4,5,19] and neuropathy-associated deinnervation[6–9] have been linked to the abnormality of the ocular surface. These structural alterations would certainly have adverse effects on corneal epithelia. Moreover, although rapid turnover, the epithelia may also be directly targeted by prolonged hyperglycemia, resulting in the generation of reactive oxidative species and the impairment of cell function. Indeed, we previously demonstrated that epidermal growth factor receptor (EGFR), along with its two effectors extracellular signal-regulated kinase (ERK) and phosphoinositide-3 kinase (PI3K)/AKT, is pivotal for corneal epithelial wound healing.[20–24] More recently we showed that EGFR signaling is impaired by hyperglycemia in corneal epithelial cells in vitro and ex vivo.[25,26] Another common sequela in diabetic patients is punctate keratitis, which is likely due to the disruption of epithelial cell junctions, such as tight junctions and adherens junctions. These junctions play an important role in the formation and maintenance of epithelial barrier, homeostasis and host defense of the cornea.[27–30] While altered distribution and expression of tight junction proteins in diabetic retina have been well documented,[31,32] the effects of hyperglycemia in inducing the breakdown of corneal epithelium remain elusive.

In the present study, we documented the corneal complications in STZ-induced DM rats, including general ocular surface health, tear secretion, corneal innervation, and epithelial wound healing. We also showed that EGFR signaling was altered and cell-cell junction formation after an epithelial injury was delayed in diabetic corneas. These results shed new light on the understanding of the pathogenesis of DK and/or epitheliopathy.

From the Kresge Eye Institute, Departments of Ophthalmology and Anatomy and Cell Biology, Wayne State University School of Medicine, Detroit, Michigan.

Supported by grants from the National Institutes of Health R01EY10869 and EY17960 (F-SXY), Research to Prevent Blindness (Department of Ophthalmology, Wayne State University), and Alliance for Vision Research (JY).

Submitted for publication April 8, 2011; revised June 15, 2011; accepted June 16, 2011.

Disclosure: **J. Yin**, None; **J. Huang**, None; **C. Chen**, None; **N. Gao**, None; **F. Wang**, None; **F.-S.X. Yu**, None

Corresponding author: Fu-Shin X. Yu, Kresge Eye Institute, Wayne State University School of Medicine, 4717 St. Antoine Boulevard, Detroit, MI, 48201; fyu@med.wayne.edu.

METHODS

Materials

Phospho (p)-EGFR (Tyr1068), AKT, and pAKT (Ser473) antibodies were from Cell Signaling (Danvers, MA). P-ERK1/2 (p42/p44), ERK2 (p42 MAPK), EGFR, and actin antibodies were from Santa Cruz Biotechnology (Santa Cruz, CA). β-catenin, ZO-1 and occludin antibodies were from BD Biosciences (San Jose, CA), Invitrogen (Carlsbad, CA), and Zymed Laboratory (South San Francisco, CA), respectively. Horseradish peroxidase conjugate secondary antibodies were from Bio-Rad (Hercules, CA). FITC conjugate secondary antibodies were from Jackson ImmunoResearch Laboratories (West Grove, PA). Contour glucometer was from Bayer HealthCare (Mishawaka, IN). All other reagents and chemicals were purchased from Sigma-Aldrich (St. Louis, MO).

Animals

Six-week-old male Sprague-Dawley (SD) rats, weighing approximately 150 g, were purchased from Charles River Laboratories (Wilmington, MA) and housed under standard conditions with continuously available water and chow (LabDiet 5001 Rodent Chow, Dexter, MI). All investigations conformed to the regulations of the ARVO Statement for the Use of Animals in Ophthalmic and Vision Research, the National Institutes of Health, and the guidelines of the Animal Investigation Committee of Wayne State University.

Induction of Diabetes and Characterization of Physical Properties in SD Rats

SD rats were randomly divided into the DM and age-matched normal control (NL) groups. Type I DM was induced with an intraperitoneal injection of 40 mg/kg of STZ in ice-cold 0.5 M citrate buffer, pH 4.5, and a second dose of 40 mg/kg STZ 24 hours later.[33] The NL group received 2 doses of intraperitoneal injection of the citrate buffer only. Serum glucose levels were monitored from rat tail vein using a glucometer. All STZ rats developed glucose levels higher than 400 mg/dL 3 days postinjection. Glucose levels and body weight were monitored weekly. At 4 and 8 weeks postinjection, body length without tails was measured and corneal diameter was measured (Castroviejo Calipers; V. Mueller, Wurmlingen, Germany).

Slit Lamp Examination

Rats were anesthetized with an intraperitoneal injection of rodent anesthesia cocktail containing 70 mg/kg ketamine and 7 mg/kg xylazine. Animals were examined with a slit lamp (Zeiss, Oberkochen, Germany) at 8 weeks post-STZ injection for corneal irregularity, defects, edema, infiltrations, and cataract while the pupils were dilated with 1% ophthalmic solution (Tropicamide Ophthalmic Solution; Akron, Buffalo Grove, IL). Corneal surface was further examined with 1% fluorescein sodium and 1% Rose Bengal staining, and photographed with a digital camera (Pentax; Golden, CO) attached to the slit lamp under Cobalt blue or red free filters, respectively. To quantitate Rose Bengal staining pattern, each cornea is divided into four quadrants and each quadrant is scored based on the following scale: 0, no staining; 1, punctate staining; 2, continuous staining covering <50% area; 3, continuous staining covering >50% area but not confluent; and 4, confluent staining. The final score for each cornea is the total of scores from all quadrants.

Evaluation of Tear Secretion and Corneal Sensitivity

Tear secretion was determined with phenol red–impregnated cotton threads (Zone-Quick, Tokyo, Japan). The threads were placed in the medial canthus for 1 minute and the length of the wetted part, turning red on soaking tears, was measured. Corneal sensation was measured with an esthesiometer (Cochet-Bonnet; Luneau, France) in unanesthetized rats. The testing began with the nylon filament fully extended to its maximal length of 60 mm and shortened by 5 mm each time a negative response was observed until a positive response was obtained. A positive blinking response was recorded by two observers and each testing was repeated three times.

Confocal Microscopic Examination

Starting at Week 2 after STZ injection, rat corneas were scanned with a digital confocal scanning microscope (ConfoScan-4; Nidek Technologies, Gamagori, Japan). Topical proparacaine 0.5% (Akron) was applied to the cornea of anesthetized rats. A drop of GenTeal gel was applied to the tip of a 40× objective lens and the central cornea was scanned using the Auto Full mode at 25 frames per second with scan step of 5 μm and total of 350 images. Each cornea was scanned three times and the corneal thickness was calculated as the peak to peak distance in the z-scan profile and averaged among three scans. To analyze corneal innervation, three representative images of the subbasal nerve plexus from each rat were selected and nerve fiber length was traced and measured (NeuronJ plug-in of ImageJ software developed by Wayne Rasband, National Institues of Health, Bethesda, MD; available at http://rsb.info.nih.gov/ij/index.html). The final length for each animal is the mean of three scans and expressed in an arbitrary unit.

Determination of Corneal Epithelial Wound Healing

Topical proparacaine 0.5% was applied to NL and DM rat corneas 8 weeks after STZ injection. A 5-mm circular wound was first demarcated with a trephine in the central cornea and the epithelium was then removed with a blunt scalpel blade under a dissecting microscope (Zeiss). Bacitracin ophthalmic ointment (Fougera, Melville, NY) was applied to the cornea after surgery to prevent infection. To document the healing process, the remaining denuded area was visualized with fluorescein staining, photographed, and quantitated (Photoshop, version 6; Adobe, San Jose, CA). Healing rate was calculated as (original wound area − current wound area)/original wound area in percentage.

Determination of Protein Expression by Western Blot Analysis

The epithelium removed during corneal debridement was lysed with radioimmunoprecipitation assay buffer (RIPA). Protein concentrations were determined using a protein assay kit (Micro BCA; Pierce, Rockford, IL). Levels of various proteins were determined using specific antibodies. Densitometry was measured with image analysis software (Kodak 1 D).

Histopathology and Immunohistochemistry

To determine histologic changes, unwounded corneas from DM or NL rats 8 weeks after STZ injection were fixed in 4% paraformaldehyde, paraffin-embedded, stained with hematoxylin and eosin, and photographed. Corneas at various time points postwounding were embedded (OCT; Ted Pella, Inc., Redding, CA), snap frozen, and cryostat-sectioned for immunofluorescence staining. The slides were fixed in 4% paraformaldehyde, blocked with bovine serum albumin, incubated with primary antibody or mouse or rabbit IgG isotype controls overnight at 4°C, followed by incubation with FITC-conjugated secondary antibody. The slides were then washed in PBS and mounted with mounting medium (Vectashield; Vector Labs, Burlingame, CA) with DAPI for nuclear staining and examined under a fluorescence microscope (Carl Zeiss Axioplan 2 equipped with an ApoTome digital camera). Negative controls (mouse or rabbit IgG isotypes) exhibited no fluorescence (data not shown).

Statistical Analysis

Each experiment used $n = 8$–10 rats in each group, NL or DM, unless otherwise noted in the figure legends. Results are mean ± SEM. Statistical parameters were ascertained (SigmaStat; Systat Software, San

Jose, CA) with Student's *t*-test between two groups. $P < 0.05$ indicates a significant difference.

Results

Maintenance of Hyperglycemia and Attenuation of Growth

The blood sugar levels were approximately 100 mg/dL in vehicle-injected normal control (NL) and higher than 500 mg/dL in STZ diabetic (DM) rats (Fig. 1A). While NL rats maintained a steady weight gain, 2.7- and 3.4-fold increases over the initial weight at 4 and 8 weeks postinjection; the body weight of STZ-rats increased only 2.1- and 2.2-fold and were 23% and 36% lower than that of the controls. The body length was also decreased, but to a lesser extent, 15% and 12% at these two time points (Fig. 1C). The DM rats also exhibited adipose and muscle tissue wasting, polyuria, polydypsia, and some exhibited diarrhea and intestinal bloating.

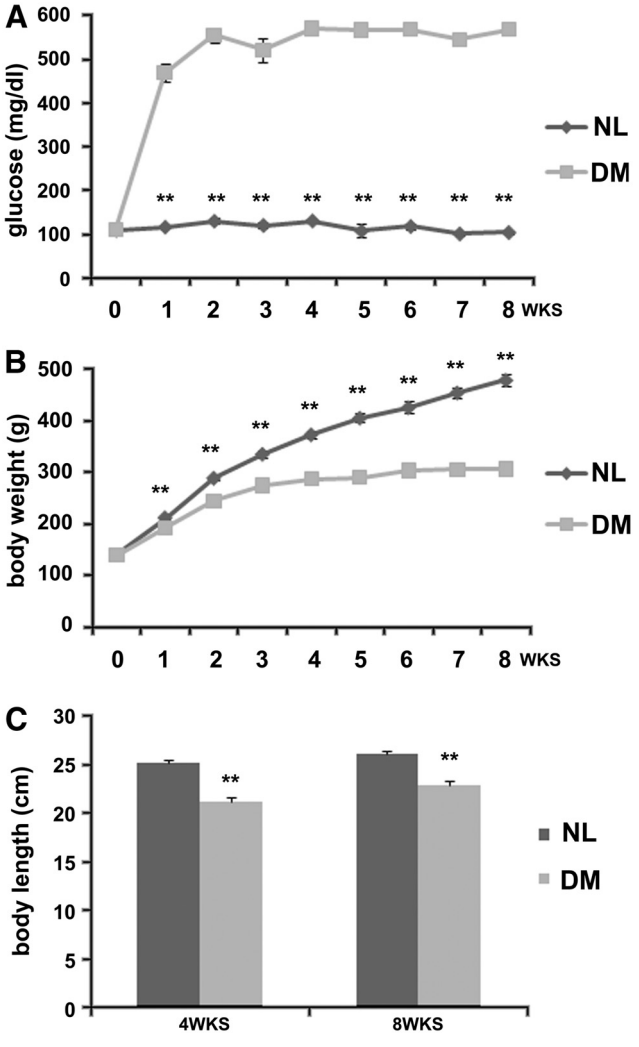

Figure 1. Hyperglycemia and growth retardation in DM rats. Six-week-old male SD rats were intraperitoneally injected with two doses of 40 mg/kg STZ diluted in citrate buffer (DM). Age-matched control rats (NL) received citrate buffer injection only. (**A**) Blood glucose was measured weekly, $^{**}P < 0.001$. (**B**) Body weight was measured weekly, $^{**}P < 0.001$. (**C**) The length of the body without tail was measured at 4 and 8 weeks postinjection, $^{**}P < 0.001$.

Alterations in Ocular Properties

To characterize the ocular changes caused by hyperglycemia, DM and NL rats were subjected to a battery of ophthalmic examinations and measurements. Unlike the body weight and length, the corneal size of DM rats was only slightly smaller than that of the controls, 5.50 mm versus 5.79 mm, a 5% decrease in diameter at 8 weeks of DM (Fig. 2A). No gross difference in histology was observed (Fig. 2B). Slit lamp examination revealed no significant ocular irregularity or epithelial morphologic changes (Fig. 2C). Fluorescein staining of the cornea revealed no visible defects (Fig. 2D). DM rats started showing lens opacity around 3 weeks of hyperglycemia and by 8 weeks nearly 100% of the DM rats developed cataract (Fig. 2C); while the lenses of the NL rats remained clear.

Rat corneas were also examined with confocal microscopy (ConfoScan; Nidek Technologies; Fig. 2E). The morphology of corneal epithelium, stroma (data not shown), and endothelium was compared between the two groups, and no significant differences were noted. Corneal thickness (Fig. 2F) was similar between NL and DM rats, averaging approximately 170 μm.

Attenuation of Tear Film Protection and Tear Secretion

The rat corneas of DM and NL rats were stained with Rose Bengal, a dye commonly used to visualize conjunctiva but also useful in highlighting tear film impairment.[34] Unlike ocular surface fluorescein staining that showed no difference between NL and DM rats, Rose Bengal staining was much stronger in the DM rats than that in the controls (Fig. 3A). The staining was quantitated as described in the Methods section and DM rats scored 7.5, higher than the 1.75 score of NL rats, indicating a deficiency of tear film protection (Fig. 3B). Tear secretion was measured with cotton threads. Consistent with Rose Bengal staining deficiency, DM rats had significantly reduced amount of tears than that of the NL rats (Fig. 3C).

Impairment of Corneal Sensitivity and Innervation

Corneal sensitivity was determined with an esthesiometer and the values were expressed as the length of the esthesiometer thread in centimeters with 6 being the longest or most sensitive (Fig. 4A). Seventy-five percent of NL rats and 58% of DM rats showed a positive blinking response at 6 cm and on average DM rats exhibited a slight yet significant decrease in sensitivity. To visualize corneal innervation, the subbasal plexus of nerve fibers was assessed with confocal microscopy (ConfoScan; Nidek Technologies). Compared with the NL rats, the nerve fibers of the DM rats are thinner and have fewer branches (Fig. 4B). The length of the nerves in each frame was calculated; and Figure 4C shows a significant reduction from 13 arbitrary units of the NL to four in the DM.

Delay in Epithelial Wound Healing

A 5-mm wound was made in the center of the cornea, leaving the limbal region intact. The healing progress was monitored with fluorescein staining to highlight denuded area and photographed (Fig. 5A). The healing rate was calculated and shown in Figure 5B. The NL rats healed 66%, 90%, 94%, and 100% at 24, 32, 40, and 48 hours postwounding (hpw), while the DM rats healed 51%, 66%, 83%, and 90%. More than one third of NL corneas completely closed the wound by 40 hpw and 100% by 48 hpw; while only one third of DM corneas healed completely by 48 hpw.

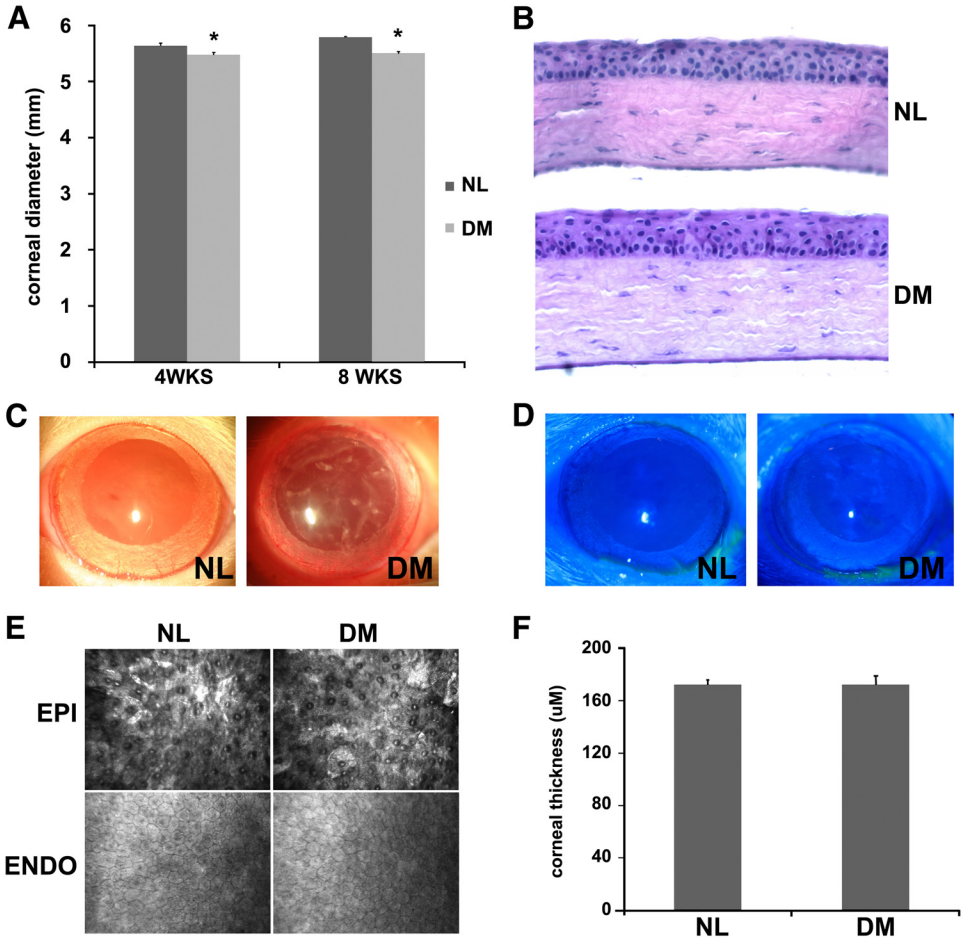

Figure 2. Ocular properties in DM rats. (**A**) Corneal diameter was measured at 4 and 8 weeks post-STZ injection, $^{*}P < 0.05$. (**B**) Eight weeks postinjection, corneas were cut in cross-section and stained with hematoxylin and eosin (H&E). (**C**) Rat corneas were dilated and examined with a slit lamp to show cataract in the diabetics. (**D**) Corneas were stained with 1% fluorescein to show the absence of epithelial defect. (**E**) Rat corneas were evaluated with a confocal microscope (ConfoScan; Nidek Technologies) and representative images of the corneal epithelium and endothelium were shown. (**F**) Corneal thickness was calculated using confocal microscopy, $P = 0.99$.

Attenuation of EGFR Signaling

We previously demonstrated the critical role of EGFR signaling in corneal epithelial wound healing and homeostasis. Using Western blot analysis, we confirmed these observations and showed that the phosphorylation (activation) of EGFR, and its two downstream effectors AKT and ERK, was significantly diminished in the corneal epithelia collected from rats of 8 weeks DM, compared with the controls (Figs. 6A and 6B). The expression of total proteins of EGFR, AKT, and ERK was also slightly lower with no statistical differences. We further extended our study to AKT activation and distribution via immu-

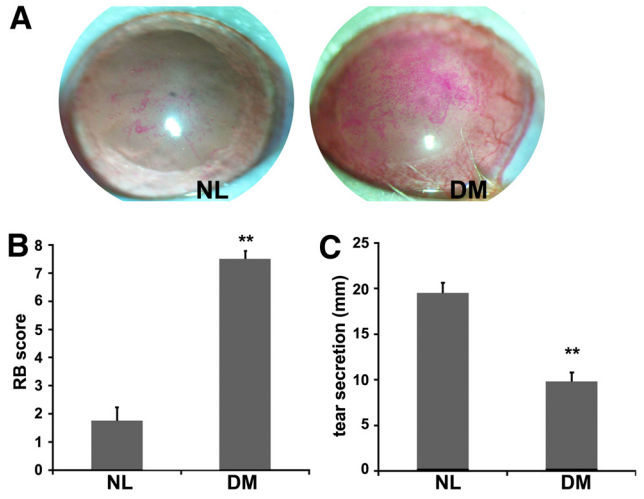

Figure 3. Impairment of tear film protection and tear secretion in DM rats. (**A**) Rat corneas were stained with Rose Bengal and representative images are shown. (**B**) Rose Bengal staining was scored, $^{**}P < 0.001$, $n = 4$. (**C**) Tear secretion was measured with cotton threads, $^{**}P < 0.001$.

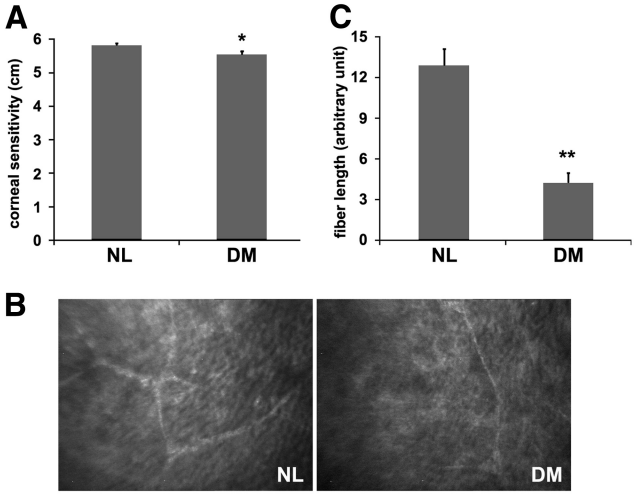

Figure 4. Impaired innervation in DM rats. (**A**) Corneal sensitivity was measured with an esthesiometer, $^{**}P < 0.05$, $n = 12$. (**B**) Subbasal plexus was visualized with confocal microscopy (ConfoScan; Nidek Technologies) and representative images are shown. (**C**) Nerve fiber length was quantitated, $^{**}P < 0.001$.

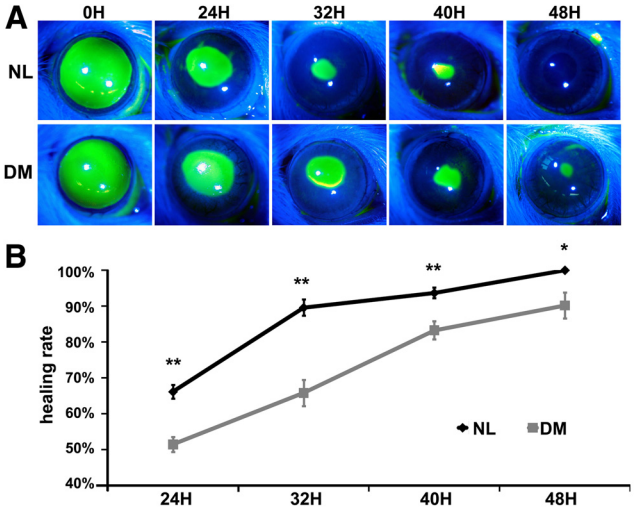

FIGURE 5. Attenuated wound healing in diabetic corneas. A 5-mm wound was made in the center of the cornea and the healing process was visualized with fluorescein staining to highlight the denuded area. Representative images are shown in (**A**). (**B**) Healing rate was calculated, $^{**}P < 0.001$ at 24, 32, and 40 hours, $^{*}P < 0.05$ at 48 hours.

nohistochemistry to 53 days postwounding (dpw) (Fig. 6C). Unwounded NL cornea exhibited stronger staining of phosphor-AKT compared with the DM. At 2, 4, and 11 dpw, more layers of cells positive of p-AKT staining were seen in the NL than in the DM, indicating a stronger AKT activation. After 23 dpw, the staining pattern of p-AKT was similar between the DM and NL corneas.

Disruption of Cell-Cell Junction

We also examined cell-cell junctions in the corneal epithelia. The expression of tight junction proteins ZO-1 and occludin, and adherens junction protein β-catenin was detected with Western blot analysis (Fig. 7A). The expression levels for these proteins were similar between the NL and DM corneas (Fig. 7B). The distribution of β-catenin (Fig. 7C) and ZO-1 (Fig. 7D) was then evaluated with immunohistochemistry, and no difference was observed between the unwounded NL and DM corneas. At 2 dpw, NL corneas exhibited continuous β-catenin staining in all epithelial layers and continuous ZO-1 staining in the apical layers in the central cornea; while the DM corneas showed sparse β-catenin staining in the apical layers and minimal ZO-1 staining in the central cornea. The staining pattern of β-catenin and ZO-1 was similar between the two groups in the limbal region at 2 dpw (data not shown). No significant difference in the distribution of β-catenin and ZO-1 was noticed at 7 dpw, indicative of a delayed but not absent formation of cell-cell junctions in the DM corneas.

DISCUSSION

In the present study, we investigated the ocular surface alterations in STZ-induced hyperglycemic rats, in comparison with age-matched normoglycemic rats. We showed that unlike body weight and length, the size of STZ-rat cornea was reduced only slightly. Slit lamp examinations for surface irregularity, punctate keratitis, or fluorescein staining as well as histologic examination for morphology revealed no detectable differences between hyperglycemic and normoglycemic rats. Rose Bengal staining was greatly increased in diabetic corneas, together with reduced tear secretion, which suggests a tear film dysfunction. Corneal sensitivity was decreased slightly but significantly. Confocal microscopy (ConfoScan; Nidek Technologies) examination showed no difference in the thickness and the morphology of all three cellular layers, but revealed thinner, less abundant subbasal nerve plexuses with fewer branches in the diabetic corneas. Consistent with studies reported by us and others,[35–38] the healing of epithelial debridement wound was significantly delayed in diabetic corneas. The phosphorylation of EGFR, AKT, and ERK was decreased in unwounded corneal epithelium and the distribution of active AKT was altered during and after wound healing was complete. Finally, the reformation of both tight junction and adherens junction after wound closure was also delayed in the diabetic corneas. Taken together, our data showed that hyperglycemia causes multifarious alterations at the ocular surface including reduced tear secretion, decreased innervation, altered EGFR signaling, and impaired reformation of cell-cell junctions of corneal epithelia. Altered innervation and tear secretion may influence epithelial response to wounding, leading to the delay of wound healing in diabetic rat corneas.

We systematically documented the ocular alterations in diabetic rats. The corneal surface examined with a slit lamp is smooth with no significant fluorescein staining. Consistent with no visible epithelial defect, histologic analyses reveal similar morphology between diabetic and normal corneas. Staining the cornea with Rose Bengal, however, showed much stronger staining in the diabetic corneas. In humans, many patients with diabetic retinopathy have increased staining of both fluorescein and Rose Bengal staining.[5,39] Although fluorescein and Rose Bengal are frequently used together in the clinic setting, sometimes interchangeably; they actually stain for different defects.[34] While fluorescein staining manifests disruption of cell-cell junctions, Rose Bengal staining highlights a deficiency of preocular tear film protection. Hence, our data suggest that epithelial barrier in unwounded diabetic corneas was intact, but the tear film protection was weakened. Consistent with this, tear secretion measured with cotton threads was decreased in STZ rats as early as 4 weeks of diabetes (data not shown). This is consistent with human studies,[4,5,19] and may explain the increase in Rose Bengal staining. Moreover, the increase in Rose Bengal, but not fluorescein, staining suggests that the decrease in tear secretion and/or tear film stability precedes corneal epithelial surface irregularity and punctate keratitis and that tear deficiency contributes to the pathogenesis of epitheliopathy/keratopathy. Hence, Rose Bengal staining might be useful for early detection of diabetic ocular surface complication and the use of artificial tears when Rose Bengal staining is observed in diabetic patients may not only alleviate dry eye symptoms but also delay or even prevent the development of DK.

High resolution digital slit scanning confocal microscopy offers a unique means to visualize the cornea noninvasively. We scanned rat corneas using fourth-generation confocal microscopy (ConfoScan; Nidek Technologies) 8 weeks after STZ injection and observed no distinctive morphologic changes in the epithelium, stroma, and endothelium among the diseased and control animals. Corneal thickness, calculated from the images, was approximately 170 μm in both the NL and DM rats, and similar to the 160 μm reported previously using an optical low coherence reflectometer.[40] Human studies showed a thickening of the cornea in diabetic patients.[12–14] The discrepancy is likely due to the durations of hyperglycemia or DM and/or species difference. The 8-week STZ may represent an early stage of human type 1 DM because rats at this time point show no detectable capillary changes and no signs of complications such as diabetic retinopathy.[41] This was also supported by the increased Rose Bengal, but not fluorescein, staining of the rat cornea.

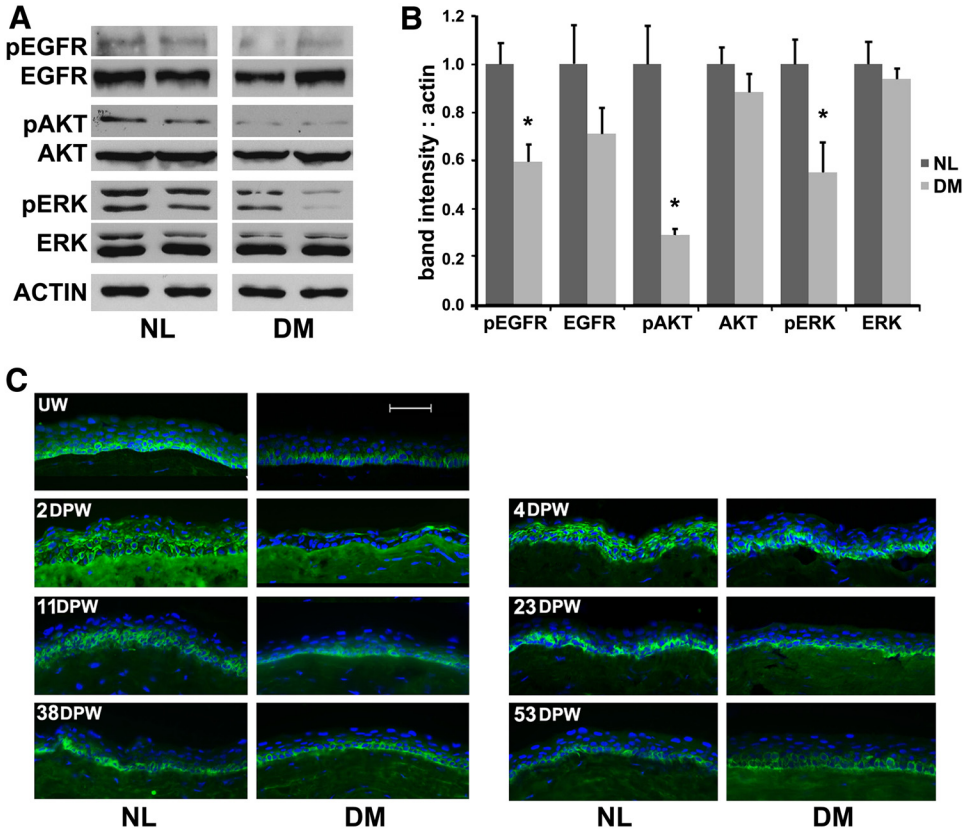

Figure 6. Impaired EGFR signaling in diabetic corneas. Rat corneal epithelium was processed for Western blot analysis, and actin serves as a loading control. (**A**) Representative images are shown. (**B**) Densitometry was measured and expressed as mean ± SEM ($n = 3$), $^*P < 0.05$. (**C**) Cryostat sections of rat corneas, unwounded (uw) or various days postwounding, were immunostained for phospho-AKT (FITC, green) and the nuclei (DAPI, blue), magnification, ×200, scale bar, 50 μm.

While 8-week STZ rats have no clinically detectable structural abnormality of the cornea or retinopathy,[41] our study revealed a slight, statistically insignificant, decrease in corneal sensitivity at 4 weeks post-STZ (data not shown) and a statistically significant decrease at 8 weeks, suggesting potential damage of some nerve ends of sensory neurons as early as 4 weeks of consistent hyperglycemia (>450 mg/dL). The value of the decrease in 8-week STZ rats was small, 0.27 cm or <5% in the length of the nylon filament. This low value may be related to the fact that SD rats are extremely sensitive to the

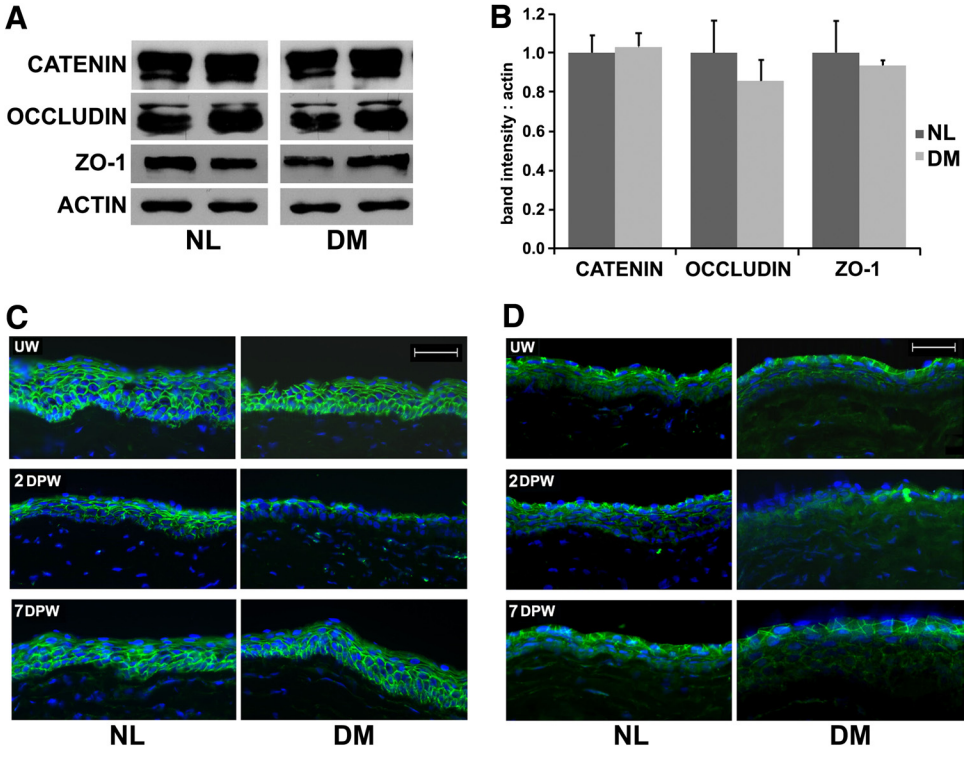

Figure 7. Disrupted formation of cell junctions in diabetic corneas. Rat corneal epithelium was processed for Western blot analysis, and actin serves as a loading control. (**A**) Representative images are shown. (**B**) Densitometry was measured and expressed as mean ± SEM ($n = 3$); no statistical difference between NL and DM. Cryostat sections of central corneas, unwounded (uw), 2 and 7 days postwounding (dpw) were immunostained for β-catenin (**C**) and ZO-1 (**D**), FITC green. Nuclei are stained with DAPI, blue. Magnification, ×200, scale bar, 50 μm.

esthesiometer, making the detection of potential difference in those rats with 6 cm readings unfeasible. It is interesting to mention that Wistar rats at 3 months of age are responsive to 5 cm or shorter and most Goto-Kakizaki rats, a type 2 DM model selected from the Wistar rats, at the same age (6 weeks of hyperglycemia) are unresponsive to 1 cm (Yu F-S, unpublished data, 2011). Consistent with reduced corneal sensitivity, diabetic rats started showing thinning and shortening of subbasal plexuses, viewed with confocal microscopy, as early as 4 weeks of DM, although nerve fiber length comparison failed to show a statistical difference (data not shown). Eight weeks post-STZ, reduction in innervation was prominent in diabetic rats. This is consistent with the literature and findings in human subjects.[9,42,43] It is interesting to note that the reduction of long nerve fibers precedes reduction in mechanical sensitivity measured with an esthesiometer,[44] suggesting that confocal microscopy may be more sensitive in detecting early changes in corneal neuropathy. It has been suggested that peripheral neuropathy affects lacrimal gland function in diabetes, thus reducing tear protection.[6] Hence, hyperglycemia-caused loss of sensory neurons and neurotrophic keratopathy may affect surrounding epithelia adversely in two ways: directly by reducing the release of epithelium-nourishing neuron peptides, and indirectly through influencing lacrimal gland function.

Indeed, although hyperglycemia-induced alterations in unmanipulated corneal epithelium are subtle and undetectable, we showed the healing of epithelial debridement wound in the cornea of 8-week STZ rats was impaired. Unlike our previous study that used weight-matched 6-month STZ rats,[38] we chose age-matched controls in this study as did most studies in the literature.[45,46] Choosing a proper control for wound healing study in diabetic corneas presents a dilemma. On the one hand, age-matched controls are bigger in the sizes of the body and the cornea; on the other hand, weight-matched controls are younger in age, albeit the age of neither group (7.5 months old for diabetic and 4.5 for normal controls) we used is considered advanced. Our studies suggest although both size and age factors can potentially confound the findings, epithelial wound healing is delayed in both scenarios.

The healing response in normal corneas is tightly regulated[47–49] and many epithelial defects and abnormalities have been suggested to be related to alterations in EGFR signaling,[50,51] critical in cell migration, adhesion, proliferation, cytoskeletal rearrangement, and wound healing.[20,23,24,52] We examined the expression and activation (phosphorylation) of EGFR, AKT, and ERK in the corneal epithelium and showed that while the total protein levels remain relatively unchanged, their phosphorylation is reduced in unwounded diabetic corneas. This is consistent with our previous study showing diminished responses of EGFR activation in normal and the migrating corneal epithelia.[38] There is multiple-layer distribution of active AKT in the normal corneal epithelium from 2 dpw to 23 dpw, while there is only basal distribution in the diabetic, suggesting that p-AKT may play a role in cell proliferation, differentiation, and even cell junction formation after injury. Echoing our findings are the observations that inhibiting EGFR function with cetuximab and gefitinib for cancer treatments resulted in ocular abnormalities in patients, including diffuse punctate keratitis and corneal erosion[53–56] and that ulcerative keratitis occurs in gastrointestinal cancer patients taking perifosine, an AKT inhibitor.[57] While the effects of hyperglycemia on wound healing apparatus, such as cytoskeleton and integrin-mediated cell adhesion, remain undetermined, this study, along with our recent publications,[38] indicates that the impaired or blunted EGFR signaling response to injury is a major cause for delayed epithelial wound healing seen in diabetic rat and human corneas.

Cell junction plays an important role in the formation and maintenance of epithelial barrier and homeostasis in many epithelia including the cornea.[27–30] In humans, punctate keratitis is observed in some diabetic patients,[2,58] suggesting defects in epithelial junctions, especially the tight junctions. However, to date the effects of hyperglycemia on corneal epithelial junctions have not been extensively studied. We showed that the expression of tight junction protein ZO-1 and occludin and adherens junction protein β-catenin was unaltered by diabetes in the unwounded cornea. ZO-1 was distributed in the apical layer in a similar pattern between unwounded NL and DM corneas; while β-catenin was distributed throughout the entire corneal thickness and its staining is also similar between unwounded NL and DM. These observations are consistent with no punctuate fluorescent staining in 8-week STZ rats. Interestingly, 2 days postwounding, the staining of ZO-1 and β-catenin was weak, discontinuous, and sparse in the diabetic corneas. By 7 dpw, the staining pattern was similar again between the two groups, suggesting that reformation of cell junctions is delayed but not absent during diabetes.

In summary, 8 weeks of continual hyperglycemia affects ocular surface tissues, lacrimal glands, and the nervous system in rats. Effective treatment of DK and delayed wound healing may require multiple medications targeting different components of the ocular surface.

References

1. Clark CM, Lee DA. Prevention and treatment of the complications of diabetes mellitus. *N Engl J Med.* 1995;332:1210–1217.
2. Schultz RO, Van Horn DL, Peters MA, Klewin KM, Schutten WH. Diabetic keratopathy. *Trans Am Ophthalmol Soc.* 1981;79:180–199.
3. Kaji Y. Prevention of diabetic keratopathy. *Br J Ophthalmol.* 2005; 89:254–255.
4. Goebbels M. Tear secretion and tear film function in insulin dependent diabetics. *Br J Ophthalmol.* 2000;84:19–21.
5. Ozdemir M, Buyukbese MA, Cetinkaya A, Ozdemir G. Risk factors for ocular surface disorders in patients with diabetes mellitus. *Diabetes Res Clin Pract.* 2003;59:195–199.
6. Cousen P, Cackett P, Bennett H, Swa K, Dhillon B. Tear production and corneal sensitivity in diabetes. *J Diabetes Complications.* 2007;21:371–373.
7. Dogru M, Katakami C, Inoue M. Tear function and ocular surface changes in noninsulin-dependent diabetes mellitus. *Ophthalmology.* 2001;108:586–592.
8. Saito J, Enoki M, Hara M, Morishige N, Chikama T, Nishida T. Correlation of corneal sensation, but not of basal or reflex tear secretion, with the stage of diabetic retinopathy. *Cornea.* 2003; 22:15–18.
9. Messmer EM, Schmid-Tannwald C, Zapp D, Kampik A. In vivo confocal microscopy of corneal small fiber damage in diabetes mellitus. *Graefes Arch Clin Exp Ophthalmol.* 2010;248:1307–1312.
10. Siribunkum J, Kosrirukvongs P, Singalavanija A. Corneal abnormalities in diabetes. *J Med Assoc Thai.* 2001;84:1075–1083.
11. Taylor HR, Kimsey RA. Corneal epithelial basement membrane changes in diabetes. *Invest Ophthalmol Vis Sci.* 1981;20:548–553.
12. Lee JS, Oum BS, Choi HY, Lee JE, Cho BM. Differences in corneal thickness and corneal endothelium related to duration in diabetes. *Eye (Lond).* 2006;20:315–318.
13. Akinci A, Bulus D, Aycan Z, Oner O. Central corneal thickness in children with diabetes. *J Refract Surg.* 2009;25:1041–1044.
14. Sahin A, Bayer A, Ozge G, Mumcuoglu T. Corneal biomechanical changes in diabetes mellitus and their influence on intraocular pressure measurements. *Invest Ophthalmol Vis Sci.* 2009;50: 4597–4604.
15. Brightbill FS, Myers FL, Bresnick GH. Postvitrectomy keratopathy. *Am J Ophthalmol.* 1978;85:651–655.

16. Schulze SD, Sekundo W, Kroll P. Autologous serum for the treatment of corneal epithelial abrasions in diabetic patients undergoing vitrectomy. *Am J Ophthalmol.* 2006;142:207–211.
17. Azar DT, Spurr MSJ, Tisdale AS, Gipson IK. Altered epithelial-basement membrane interactions in diabetic corneas. *Arch Ophthalmol.* 1992;110:537–540.
18. McDermott AM, Xiao TL, Kern TS, Murphy CJ. Non-enzymatic glycation in corneas from normal and diabetic donors and its effects on epithelial cell attachment in vitro. *Optometry.* 2003;74:443–452.
19. Akinci A, Cetinkaya E, Aycan Z. Dry eye syndrome in diabetic children. *Eur J Ophthalmol.* 2007;17:873–878.
20. Xu KP, Ding Y, Ling J, Dong Z, Yu FS. Wound-induced HB-EGF ectodomain shedding and EGFR activation in corneal epithelial cells. *Invest Ophthalmol Vis Sci.* 2004;45:813–820.
21. Xu KP, Riggs A, Ding Y, Yu FS. Role of ErbB2 in corneal epithelial wound healing. *Invest Ophthalmol Vis Sci.* 2004;45:4277–4283.
22. Xu KP, Yin J, Yu FS. SRC-family tyrosine kinases in wound- and ligand-induced epidermal growth factor receptor activation in human corneal epithelial cells. *Invest Ophthalmol Vis Sci.* 2006;47:2832–2839.
23. Xu KP, Yin J, Yu FS. Lysophosphatidic acid promoting corneal epithelial wound healing by transactivation of epidermal growth factor receptor. *Invest Ophthalmol Vis Sci.* 2007;48:636–643.
24. Yin J, Xu K, Zhang J, Kumar A, Yu FS. Wound-induced ATP release and EGF receptor activation in epithelial cells. *J Cell Sci.* 2007;120:815–825.
25. Xu KP, Li Y, Ljubimov AV, Yu FS. High glucose suppresses EGFR-PI3K-AKT signaling pathway and attenuates corneal epithelial wound healing. *Diabetes.* 2009.
26. Yin J, Yu FS. LL-37 Promotes high glucose-attenuated epithelial wound healing via EGFR transactivation in organ cultured corneas. *Invest Ophthalmol Vis Sci.* 2009.
27. Gudmundsson OG, Ormerod LD, Kenyon KR, et al. Factors influencing predilection and outcome in bacterial keratitis. *Cornea.* 1989;8:115–121.
28. Sugrue SP, Zieske JD. ZO1 in corneal epithelium: association to the zonula occludens and adherens junctions. *Exp Eye Res.* 1997;64:11–20.
29. Suzuki K, Tanaka T, Enoki M, Nishida T. Coordinated reassembly of the basement membrane and junctional proteins during corneal epithelial wound healing. *Invest Ophthalmol Vis Sci.* 2000;41:2495–2500.
30. Yin J, Yu FS. Rho kinases regulate corneal epithelial wound healing. *Am J Physiol Cell Physiol.* 2008;295:C378–387.
31. Barber AJ, Antonetti DA, Gardner TW. Altered expression of retinal occludin and glial fibrillary acidic protein in experimental diabetes. The Penn State Retina Research Group. *Invest Ophthalmol Vis Sci.* 2000;41:3561–3568.
32. Klaassen I, Hughes JM, Vogels IM, Schalkwijk CG, Van Noorden CJ, Schlingemann RO. Altered expression of genes related to blood-retina barrier disruption in streptozotocin-induced diabetes. *Exp Eye Res.* 2009;89:4–15.
33. Zagon IS, Sassani JW, Myers RL, McLaughlin PJ. Naltrexone accelerates healing without compromise of adhesion complexes in normal and diabetic corneal epithelium. *Brain Res Bull.* 2007;72:18–24.
34. Feenstra RP, Tseng SC. Comparison of fluorescein and Rose Bengal staining. *Ophthalmology.* 1992;99:605–617.
35. Hallberg CK, Trocme SD, Ansari NH. Acceleration of corneal wound healing in diabetic rats by the antioxidant trolox. *Res Commun Mol Pathol Pharmacol.* 1996;93:3–12.
36. Zagon IS, Jenkins JB, Sassani JW, et al. Naltrexone, an opioid antagonist, facilitates reepithelialization of the cornea in diabetic rat. *Diabetes.* 2002;51:3055–3062.
37. Chikama T, Wakuta M, Liu Y, Nishida T. Deviated mechanism of wound healing in diabetic corneas. *Cornea.* 2007;26:S75–81.
38. Xu K, Yu FS. Impaired epithelial wound healing and EGFR signaling pathways in the corneas of diabetic rats. *Invest Ophthalmol Vis Sci.* 2011.
39. Yu L, Chen X, Qin G, Xie H, Lv P. Tear film function in type 2 diabetic patients with retinopathy. *Ophthalmologica.* 2008;222:284–291.
40. Schulz D, Iliev ME, Frueh BE, Goldblum D. In vivo pachymetry in normal eyes of rats, mice and rabbits with the optical low coherence reflectometer. *Vision Res.* 2003;43:723–728.
41. Kowluru RA. Effect of reinstitution of good glycemic control on retinal oxidative stress and nitrative stress in diabetic rats. *Diabetes.* 2003;52:818–823.
42. Erie EA, McLaren JW, Kittleson KM, Patel SV, Erie JC, Bourne WM. Corneal subbasal nerve density: a comparison of two confocal microscopes. *Eye Contact Lens.* 2008;34:322–325.
43. Midena E, Cortese M, Miotto S, Gambato C, Cavarzeran F, Ghirlando A. Confocal microscopy of corneal sub-basal nerve plexus: a quantitative and qualitative analysis in healthy and pathologic eyes. *J Refract Surg.* 2009;25:S125–S130.
44. Rosenberg ME, Tervo TM, Immonen IJ, Muller LJ, Gronhagen-Riska C, Vesaluoma MH. Corneal structure and sensitivity in type 1 diabetes mellitus. *Invest Ophthalmol Vis Sci.* 2000;41:2915–2921.
45. Nakamura M, Kawahara M, Morishige N, Chikama T, Nakata K, Nishida T. Promotion of corneal epithelial wound healing in diabetic rats by the combination of a substance P-derived peptide (FGLM-NH2) and insulin-like growth factor-1. *Diabetologia.* 2003;46:839–842.
46. Zagon IS, Sassani JW, McLaughlin PJ. Insulin treatment ameliorates impaired corneal reepithelialization in diabetic rats. *Diabetes.* 2006;55:1141–1147.
47. Lu L, Reinach PS, Kao WW. Corneal epithelial wound healing. *Exp Biol Med.* 2001;226:653–664.
48. Kurpakus-Wheater M, Kernacki KA, Hazlett LD. Maintaining corneal integrity how the "window" stays clear. *Prog Histochem Cytochem.* 2001;36:185–259.
49. Netto MV, Mohan RR, Ambrosio R Jr, Hutcheon AE, Zieske JD, Wilson SE. Wound healing in the cornea: a review of refractive surgery complications and new prospects for therapy. *Cornea.* 2005;24:509–522.
50. Chua BH, Chua CC, Zhao ZY, Krebs CJ. Estrone modulates the EGF receptor in the liver of db/db mouse. *J Recept Res.* 1991;11:941–957.
51. Wassef L, Kelly DJ, Gilbert RE. Epidermal growth factor receptor inhibition attenuates early kidney enlargement in experimental diabetes. *Kidney Int.* 2004;66:1805–1814.
52. Yin J, Yu FS. ERK1/2 mediate wounding- and G-protein-coupled receptor ligands-induced EGFR activation via regulating ADAM17 and HB-EGF shedding. *Invest Ophthalmol Vis Sci.* 2009;50:132–139.
53. Fukuoka M, Yano S, Giaccone G, et al. Multi-institutional randomized phase II trial of gefitinib for previously treated patients with advanced non-small-cell lung cancer (The IDEAL 1 Trial) [corrected]. *J Clin Oncol.* 2003;21:2237–2246.
54. Shah NT, Kris MG, Pao W, et al. Practical management of patients with non-small-cell lung cancer treated with gefitinib. *J Clin Oncol.* 2005;23:165–174.
55. Foerster CG, Cursiefen C, Kruse FE. Persisting corneal erosion under cetuximab (Erbitux) treatment (epidermal growth factor receptor antibody). *Cornea.* 2008;27:612–614.
56. Specenier P, Koppen C, Vermorken JB. Diffuse punctate keratitis in a patient treated with cetuximab as monotherapy. *Ann Oncol.* 2007;18:961–962.
57. Shome D, Trent J, Espandar L, et al. Ulcerative keratitis in gastrointestinal stromal tumor patients treated with perifosine. *Ophthalmology.* 2008;115:483–487.
58. Inoue K, Okugawa K, Amano S, et al. Blinking and superficial punctate keratopathy in patients with diabetes mellitus. *Eye (Lond).* 2005;19:418–421.